

Near-field visualization of light confinement in a photonic crystal microresonator

Patrick Kramper

*Centre Nationale de la Recherche Scientifique, Laboratoire de Photonique et de Nanostructures, Route de Nozay,
91460 Marcoussis, France*

Maria Kafesaki

Research Center of Crete, Heraklion, Crete, Greece

Costas M. Soukoulis

*Ames Laboratory, Iowa State University, Ames, Iowa 50011, and
Research Center of Crete, Heraklion, Crete, Greece*

Albert Birner

Infineon Technologies, Memory Products, Königsbrückerstrasse 94, 01099 Dresden, Germany

Frank Müller and Ulrich Gösele

Max-Planck-Institut für Mikrostrukturphysik, Weinberg 2, 06120 Halle, Germany

Ralf B. Wehrspohn

Nanophotonic Materials Group, Paderborn University, 33098 Paderborn, Germany

Jürgen Mlynek

President, Humboldt-Universität zu Berlin, 10099 Berlin, Germany

Vahid Sandoghdar

Laboratory of Physical Chemistry, Swiss Federal Institute of Technology, CH-8093 Zurich, Switzerland

Received July 8, 2003

By using scanning near-field optical microscopy, we directly map the subwavelength confinement of light around a point defect in a two-dimensional photonic crystal microresonator. Comparison of our results with the outcome of three-dimensional finite-difference time domain calculations allows us to identify small imperfections in the structure that result in the spatial modification of the intensity distribution. © 2004 Optical Society of America

OCIS codes: 130.0130, 270.5580, 250.0250.

The wave fronts of light in a photonic crystal (PC) undergo substantial modulations on length scales much shorter than one wavelength. Therefore it is not possible to examine the spatial details of light propagation by conventional far-field optics. To circumvent this problem, PCs could be investigated with scanning near-field optical microscopy^{1–6} (SNOM). Indeed, in recent years SNOM has found increasingly more applications in the study of photonic devices.^{7–11} In this Letter we use near-field imaging to visualize the subwavelength confinement of light at the upper surface of a deep two-dimensional PC microresonator.

To obtain SNOM images, one needs to scatter the nonpropagating near fields on a sample by raster scanning a fine subwavelength probe at a few nanometers from its surface. The dimensions and geometry of the probe determine the resolution and the strength of the signal: A finer probe provides a higher resolution at the cost of a weaker signal and vice versa. The most widespread type of SNOM uses a metal-coated optical fiber tip with a subwavelength aperture at its end. Alternatively, an apertureless probe, such as an uncoated fiber tip, could be used to detect the evanescent waves on the sample.^{7,10}

An electron microscope image of the PC studied in this work is shown in Fig. 1a. The region of interest in our experiment is marked by the white square. A point defect in the middle together with two line defects construct a microresonator that is fed by input and output waveguides. Figure 1b schematically displays the central elements of our setup. The light from a continuous-wave optical parametric oscillator¹² is focused on the entrance facet of the first waveguide. A chemically etched single-mode uncoated fluoride glass fiber tip (probe 1) is used to locate and map the intensity distribution at the exit of the second waveguide. In a previous report¹³ we used this scheme to detect the two resonances that appear in the photonic bandgap of this structure at wavelengths of 3.621 and 3.843 μm , with quality factors of 640 and 190, respectively. In this work we add a second uncoated fiber tip (probe 2) to interrogate the evanescent field at the upper surface of the PC structure, which is 100 μm deep.

Figure 2a displays the topography signal of the part of the sample that is examined by probe 2. As shown in the inset of Fig. 1b, the tip used was not very sharp. Therefore the lateral topography resolution was low, and the individual pores were not easy to recognize.

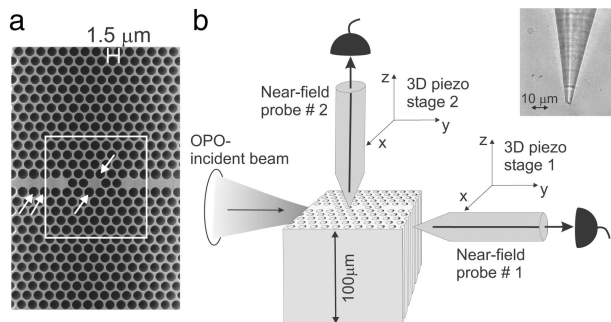


Fig. 1. a, Electron microscope image of the PC structure studied. The white square marks the area imaged by SNOM. The four arrows indicate the pores responsible for the effects discussed in Figs. 3a and 3b. b, Schematics of our setup. Two SNOM tips are used to image the light exiting the PC and the evanescent light traveling at the PC–air interface. Inset, optical micrograph of the tip. OPO, optical parametric oscillator.

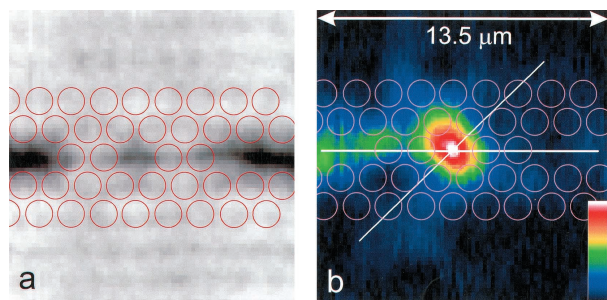


Fig. 2. a, Topography signal recorded by probe 2. b, Optical signal recorded simultaneous to the image in a. Inset, linear color code. In both a and b an array of pores is superposed to guide the eye. We note that, even though a and b were recorded simultaneously, there exists a slight lateral offset between them. This is often the case in SNOM because the sections of the tip that provide the topographic and optical signals are different. The cross sections in b are shown in Figs. 3c and 3d.

Nevertheless, the topography image clearly identifies the two waveguides as well as the point defect where the light should be confined. We used this information together with our knowledge of the scan range to overlap the PC geometry as a guide to the eye.

Figure 2b shows the raw data of the optical intensity signal recorded by probe 2 with the laser wavelength tuned to the resonance at $\lambda = 3.84 \mu\text{m}$. The subwavelength confinement of light in one dimension across the width of the waveguide and in two dimensions about the point defect is clearly evident. Furthermore, this image makes it possible to identify several interesting phenomena that cannot be accessed through spectroscopic methods. First, we note that the microresonator mode is tilted, whereas previous finite-difference time domain (FDTD) calculations showed the symmetry axes of the microcavity mode to be along the x and y directions.¹³ Second, the light is pushed to one side by a fraction of a wavelength in the last part of the input waveguide. Third, the measurements reveal subwavelength details of the intensity modulations along this waveguide. These observations indicate that the crystal parameters

might deviate slightly from their nominal values. In fact, electron microscopy studies of macroporous silicon PCs have shown that one might typically obtain fluctuations of as much as 10% in the diameters of the pores neighboring the missing pores.¹⁴ Finally, we find that the light intensity drops dramatically at the surface of the second waveguide.

To explain our experimental findings, we performed three-dimensional calculations with the FDTD method. The real space was discretized in a cubic grid with a size per grid cell of $\sim 0.11 \mu\text{m}$, and the depth of the system was taken to be $26 \mu\text{m}$. The diameters of the pores neighboring the point defect and the two line defects were taken to be 5% larger than those of the bulk PC. This was established in our previous study¹³ and is caused by a proximity effect in the electrochemical etching process during fabrication.¹⁵ The incident laser beam was considered to have a Gaussian profile with a FWHM of $6 \mu\text{m}$ and entered the PC structure with its axis placed at a depth of $4.5 \mu\text{m}$ from the PC–air interface.

FDTD simulations revealed that the intensity distribution in the waveguide and the microcavity could respond sensitively to the slightest modifications of the pores surrounding them. In Fig. 3a we plot an outcome that reproduces all the important aspects of the SNOM measurements. Here two holes surrounding the microcavity and two holes along the input waveguide (marked by arrows in Fig. 1a) are taken to be 5% smaller than the bulk value. To compare this image with its experimental counterpart in Fig. 2b, we

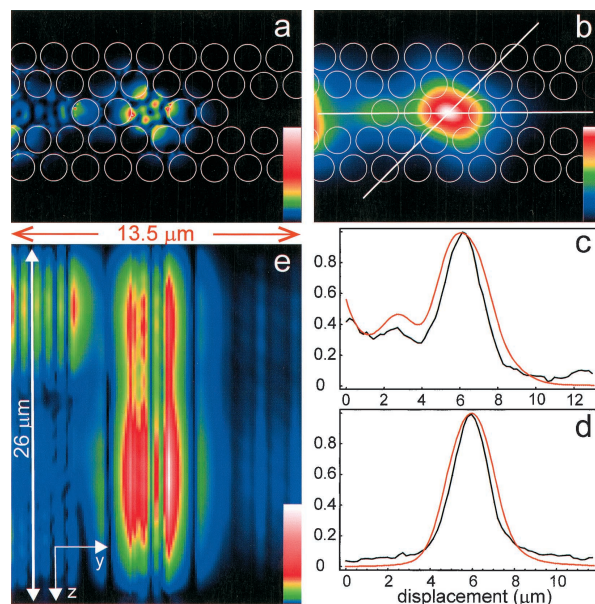


Fig. 3. a, Simulated lateral intensity distribution on the top surface if the four pores marked in Fig. 1a were to be 5% smaller than the bulk pore diameter. b, Image in a after convolution with a Gaussian filter function of FWHM = $1.4 \mu\text{m}$. c, Black and red curves show the cross sections along the waveguides through Figs. 2b and 3b, respectively. d, Corresponding diagonal cross sections through Figs. 2b and 3b. e, Cross section of the intensity distribution along the yz plane. A Gaussian beam is coupled in close to the top of the PC structure from the left-hand side.

accounted for the finite SNOM resolution by convolving the image with a Gaussian profile.¹⁶ The result is shown in Fig. 3b and has a striking resemblance to Fig. 2b. The good quantitative agreement between the two becomes clear in Figs. 3c and 3d, in which we plot two cross sections corresponding to those shown in Figs. 2b and 3b. The FWHM of the Gaussian filter function that yielded the best results was determined to be $1.4 \mu\text{m}$, implying a resolution of about $\lambda/3$. We note that since three-dimensional calculations are time consuming for deep samples, we did not exhaust the search for the perfect match between theory and experiment. As a result some residual features of the experimental data, such as the small deflection of the beam in the input waveguide and the exact tilt of the cavity mode, were not reproduced.

Another aspect of the experimental data that is verified by the simulations is the low intensity in the output waveguide, an effect that was not predicted by previous two-dimensional FDTD calculations.¹³ Figure 3e shows the in-depth intensity distribution in the yz plane along the middle of the waveguides and the point defect. After interacting with the point defect, the light was pushed downward and split into two beams. We believe this nontrivial behavior stems from a combination of surface reflections and volume diffraction of light close to the interface of a deep PC. We examined various parameters, such as the beam waist, coupling depth, and laser frequency, as well as the configuration of pore imperfections, and concluded that the details of the beam spread in the yz plane could be strongly influenced in a qualitative fashion. Here it suffices to note that the vertical beam displacement in the second waveguide resulted in much less light at the surface of the PC, which is in agreement with our experimental observation.

We now point our attention to the signal dynamics in the measurement. Although the PbSe detectors used are not very sensitive, the noise in the measurement is negligible, and we typically obtained a signal-to-noise ratio of more than 100. Furthermore, the cross sections shown in Figs. 3c and 3d allow us to put a lower limit of 20 on the signal-to-background ratio. The low scattering background is particularly noteworthy considering that we used uncoated fiber tips. We comment in passing that elimination of a propagating background light is not possible when detecting luminescence of active material embedded in the PC.^{4,6}

In conclusion, we have reported on high-resolution SNOM measurements of optical fields confined to a subwavelength two-dimensional PC microresonator. By comparing our experimental image with the outcome of the three-dimensional FDTD calculations, we have discovered slight deviations of structure parameters from their nominal values. A quantitative match between SNOM images and their numerical counterparts should be feasible for shallow PC structures, for which the numerical calculations are fast, and strong near fields at the surface allow finer SNOM probes to be used, therefore yielding higher resolution without loss of signal.

The optical measurements were performed at the University of Konstanz, with whom P. Kramper, J. Mlynek, and V. Sandoghdar were previously affiliated. This work was supported by the Deutsche Forschungsgemeinschaft (SPP 1113), Optikzentrum Konstanz, the U.S. Department of Energy, and the Information Societies Technology Program's Photonic Crystal Integrated Circuits project. We are grateful to M. Agio for numerous helpful discussions. V. Sandoghdar's e-mail address is vahid.sandoghdar@ethz.ch.

References

1. E. B. McDaniel, J. W. P. Hsu, L. S. Goldner, R. J. Tonucci, E. L. Shirley, and G. W. Bryant, *Phys. Rev. B* **55**, 10878 (1997).
2. P. L. Phillips, J. C. Knight, B. J. Mangan, P. St. J. Russell, M. D. B. Charlton, and G. J. Parker, *J. Appl. Phys.* **85**, 6337 (1999).
3. S. Fan, I. Applebaum, and J. D. Joannopoulos, *Appl. Phys. Lett.* **75**, 3461 (1999).
4. D. Gérard, L. Berguiga, F. de Fornel, L. Salomon, C. Seassal, X. Letartre, P. Rojo-Romeo, and P. Viktorovitch, *Opt. Lett.* **27**, 173 (2002).
5. S. Bozhevolnyi, V. S. Volkov, J. Arentoft, A. Boltasseva, T. Sondergaard, and M. Kristensen, *Opt. Commun.* **212**, 51 (2002).
6. K. Okamoto, M. Loncar, T. Yoshie, and A. Scherer, *Appl. Phys. Lett.* **82**, 1676 (2003).
7. J. C. Knight, N. Dubreuil, V. Sandoghdar, J. Hare, V. Lefèvre-Seguin, J. M. Raimond, and S. Haroche, *Opt. Lett.* **20**, 1515 (1995).
8. S. Bourzeix, J. M. Moison, F. Mignard, F. Barthe, A. C. Boccara, C. Licoppe, B. Mersale, M. Allovon, and A. Bruno, *Appl. Phys. Lett.* **73**, 1035 (1998).
9. M. L. M. Balistreri, H. Gersen, J. P. Korterik, L. Kuipers, and N. F. van Hulst, *Science* **294**, 1080 (2001).
10. S. Götzinger, O. Benson, and V. Sandoghdar, *Appl. Phys. B* **73**, 825 (2001).
11. V. Sandoghdar, B. Buchler, P. Kramper, S. Götzinger, O. Benson, and M. Kafesaki, in *Photonic Crystals—Advances in Design, Fabrication, and Characterization*, K. Busch, S. Lölkes, R. Wehrspohn, and H. Föll, eds. (Wiley-VCH, Weinheim, Germany, to be published).
12. K. Schneider, P. Kramper, S. Schiller, and J. Mlynek, *Opt. Lett.* **22**, 1293 (1997).
13. P. Kramper, A. Birner, M. Agio, C. M. Soukoulis, F. Müller, U. Gösele, J. Mlynek, and V. Sandoghdar, *Phys. Rev. B* **64**, 233102-1 (2001).
14. A. Birner, "Optische Wellenleiter und Mikroresonatoren in Zweidimensionalen Photonischen Kristallen aus Makroporösem Silizium," Ph.D. dissertation (Martin-Luther University at Halle-Wittenberg, Germany, 2000), available at <http://sundoc.bibliothek.uni-halle.de/diss-online/00/00H127/index.htm>.
15. A. Birner, U. Grüning, S. Ottow, A. Schneider, F. Müller, V. Lehmann, H. Föll, and U. Gösele, *Phys. Status Solidi A* **165**, 111 (1998).
16. The quantitative details of the near-field interaction between a tip and a sample depend strongly on the geometry of the tip, polarization of light, etc. and cannot be modeled in an accurate manner. Therefore we simply assume a generic Gaussian profile.